The Astrophysical Journal, 891:51 (7pp), 2020 March 1 https://doi.org/10.3847/1538-4357/ab7003

Heating of the Solar Wind by Ion Acoustic Waves

Paul J. Kellogg
University of Minnesota, MN, USA
Received 2019 June 17; revised 2020 January 22; accepted 2020 January 23; published 2020 March 3

Abstract

Calculations are made of the energy supplied to the solar wind by the rapid decay of density fluctuations, identified as ion acoustic waves. It is shown that this process supplies an appreciable fraction, perhaps nearly all, of the observed heating of the solar wind. This process may be an important step in the conversion of magnetic turbulence to particle energy.

Unified Astronomy Thesaurus concepts: Heliosphere (711); Solar wind (1534); Solar coronal heating (1989)

1. Introduction

The plasma wind from the Sun, the solar wind, is strongly accelerated near the Sun, but this heating and acceleration continues at least to 1 au. To understand this is, of course, a major goal of the recently launched *Parker Solar Probe* spacecraft, the second mission to explore this heating process near the Sun. It has been suggested (Tu & Marsch 1994, 1995; Howes et al. 2012; Narita & Marsch 2015; Verscharen et al. 2017) that the ubiquitous density fluctuations in the solar wind are waves in the ion acoustic mode, also known as the kinetic slow mode. As these are quickly turned into particle energy, it is of interest to calculate how much heating is provided and the purpose of this article is to make this calculation.

According to Vlasov calculations, ion acoustic modes are very strongly damped, with an imaginary part of the frequency of the order of a third of the real part (Barnes 1966), thus giving a damping time of the order of half a cycle. If ion acoustic waves are an important part of solar wind turbulence this poses two problems: first, why are there so many such waves when they are so evanescent; and second, is there too much heating of the solar wind? Several ways out of this perceived problem have been suggested. Howes et al. (2012) suggested that the wave vector could be very oblique, so that both the real and imaginary part of the frequency are near zero, so that absorption is slow. Tu & Marsch (1994) suggested that the Vlasov calculations are correct and that the waves were in fact absorbed, and their energy contributed to the energization and acceleration of the solar wind. A third suggestion, proposed by Schekochihin et al. (2009), Howes et al. (2006), and Parker et al. (2016), is that the Vlasov calculations do not give the correct answer for the damping in some cases.

In this article, I calculate and use in situ observations to investigate whether there are enough zero frequency waves to account for very slow absorption. It seems there are not. However, the identification of density fluctuations with the ion acoustic mode implies that the energy delivered to the ambient plasma of the solar wind by their decay is, within uncertainties, consistent with the observations of heating at 1 au. It is therefore found that the perceived problems are not problems.

It seems that the suggestion of Schekochihin and colleagues (Howes et al. 2006; Schekochihin et al. 2009; Parker et al. 2016) that the Vlasov damping is not correct in some cases is something that cannot be tested by comparison with observations, but perhaps by simulations.

2. Wave Modes

Partly for the author's own edification, a short discussion of wave mode designations follows. There are three popularly discussed wave modes in plasma. They have a dozen or two dozen names, however. Further, in Vlasov theory, there are many more modes, but only some of them correspond to MHD modes. The most popular set of names comes from MHD. The dispersion relation, the vanishing of the determinant of the MHD equations, is:

$$\omega(\omega^2 - k_z^2 V_A^2)[\omega^4 - \omega^2 k^2 (V_A^2 + V_S^2) + k^2 k_z^2 V_A^2 V_S^2] = 0. \quad (1)$$

The equation allows a fourth solution, corresponding to $\omega = 0$, which, like all $\omega = 0$ solutions, must be a pressure balanced mode. It is often ignored (though not by Verscharen et al. 2017). It is called the entropy mode or the NP (nonpropagating) mode.

The solution corresponding to the next expression in brackets will be called the shear Alfvén mode here. The remaining expression, in square brackets, corresponds to two solutions. For propagation parallel to the steady state B_0, ($k_z = k$) this is $\omega = kV_A$ and $\omega = kV_S$, where V_A and V_S are the Alfvén speed and the ion sound speed. It is usual to call the solution corresponding to $\omega = kV_S$ and its extension to oblique propagation the slow mode, although if β_w, the square of the ratio V_S/V_A, is greater than 1 it is actually faster. The corresponding Vlasov solution is called the kinetic slow mode in recent literature (the various authors have used different names for this mode). However, ion acoustic carries the suggestion that the energy of these waves is acoustic, which is true, but "kinetic" emphasizes that these waves are strongly damped, whereas they are not in MHD. In this work both names will be used. However, during much of the time analyzed in this work, the ion acoustic speed is faster than the slow speed, but the mode considered is still the highly damped mode in spite of the slow mode name. In early work and in the textbooks (e.g., Stix 1962, 1992), it was called the ion acoustic mode or the ion sound mode, but kinetic slow mode has become common in the recent literature and will also be used here. The solution corresponding to $\omega = kV_A$ for parallel propagation is called the electromagnetic ion cyclotron mode in magnetospheric work. It does not enter much in the discussion here.

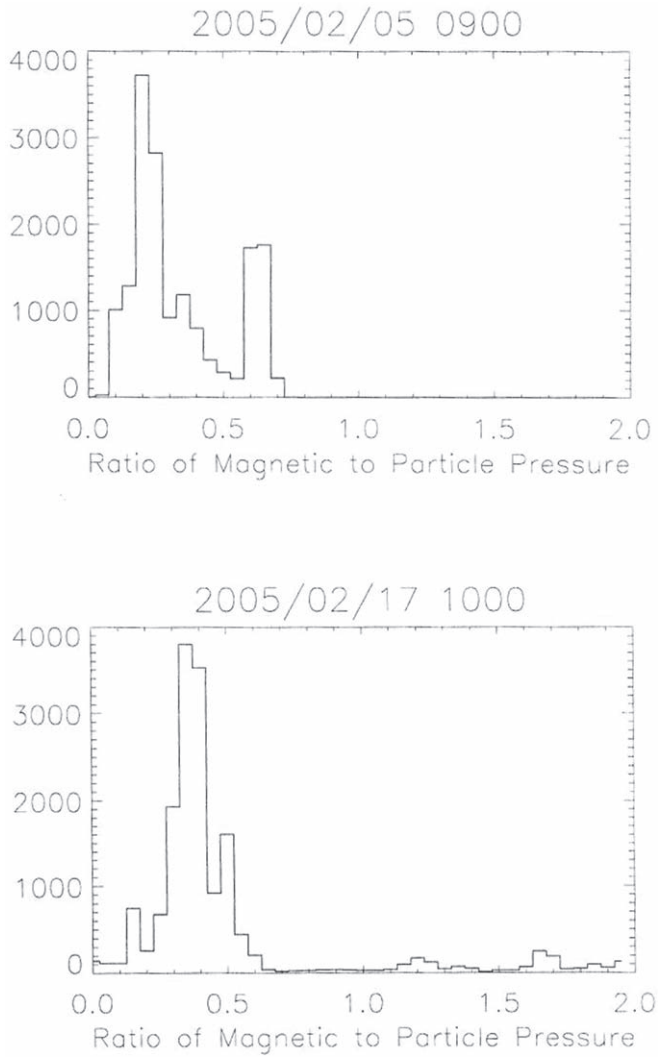

Figure 1. Histograms of the ratios of magnetic pressure to particle pressure for two periods.

2.1. $\omega = 0$ Modes

In addition to the $\omega = 0$ of the MHD equations, in the limit of extreme obliquity, i.e., the wave vector perpendicular to the ambient magnetic field, ion acoustic modes become pressure balanced modes, as must all $\omega = 0$ waves. Pressure balanced structures do occur in the solar wind (Burlaga & Ogilvie 1970a, 1970b; Tu & Marsch 1995; Vasquez & Hollweg 1999; Kellogg & Horbury 2005; Yao et al. 2011). In the solar wind, magnetic pressure is generally of the same order as particle pressure, but it appears that this is more equipartition than accurate pressure balance. Figure 1 shows two histograms of the observed ratio of magnetic pressure to particle pressure using data from the 3DP experiment (Lin et al. 1995) and the Magnetic Field Investigation experiment (Lepping et al. 1995) on *Wind*. These histograms are from two periods that have been analyzed for this work, 2005 February 5 and 17. It will be seen that accurately balanced pressures are sufficiently rare that it seems that they could not account for the common negative correlation between density fluctuations and the fluctuations of magnetic field parallel to the average magnetic field used by Howes et al. (2012) to identify ion acoustic waves.

3. Energy in Waves and Their Absorption

3.1. Some Expressions for Wave Energy

According to the solutions of the Vlasov equations for propagation parallel to the magnetic field, the imaginary part of the frequency of ion acoustic waves is of the order of one third of the real part, leading to absorption times of half a cycle (Barnes 1966). Tu & Marsch (1994, 1995) suggested, assuming that this is correct, that the energy of the waves is converted to particle energy at this rate, leading to some heating and acceleration of the solar wind. More recently, Narita & Marsch (2015) have made an extensive analysis of the Vlasov dispersion relations for these ion acoustic waves, confirming this imaginary part of the frequency but finding much change with the angle of propagation. In this article, calculations of the expected rate of such heating are presented.

There are, in the literature, several expressions for the energy in such waves. Three different approaches to the energy and the energy transferred have been tried for this work. First, in a common treatment, the wave energy is proportional to the square of the electric field fluctuations. The common expression for the energy in a wave mode which relates the energy to the electric field (Brillouin 1921; Landau & Lifshitz 1960, 1969; Auerbach 1979) is:

$$W(\omega, k) = \omega \frac{\partial \varepsilon'}{\partial \omega} \frac{\langle E(x, t)^2 \rangle}{4\pi}.$$

Here ε' is the real part of the derivative of Z, the well known electrostatic dispersion function (e.g., Fried & Conte 1961, Stix 1962, 1992) which for an electrostatic wave is the sum over species as below:

$$\varepsilon(k, \omega) = 1 - \sum_j \frac{1}{2k^2 \lambda_{Dj}^2} Z'(\zeta_j). \quad (2)$$

Second, another relation is given by Landau & Lifshitz (1960, 1969, Equation (61.4)). Third, they also give an equation for the energy transferred, not the energy, from a wave with averaged electric field E^2 in the electrostatic limit. However, all these approaches require knowledge of the mode, frequency and wavenumber of the wave being investigated. These are not known. Further, they are based on the spectrum, for which the range is also not known. This will be discussed in Section 4.2. A different approach is taken here.

In ion acoustic waves, the change in ion density almost exactly balances the change in electron density, a balance which becomes more and more perfect at lower frequencies, so that the electric field is small. Almost all of the energy is then in the acoustic system, not the electric field, which is why the name ion acoustic is mostly used here.

3.2. Acoustic Energy

Therefore the energy in ion acoustic slow mode waves will be calculated using an expression for sound waves. The energy in a sound wave (Rayleigh & Strutt 1894) is:

$$W = \text{pressure} + \text{velocity} = \int_V \frac{\partial p^2}{2\rho_0 V_S^2} dV + \int_V \frac{\rho_0 \delta v^2}{2} dV. \quad (3)$$

Here δp is the variation in pressure, ρ_0 is the average density, V_s is the speed of sound, here taken as the ion acoustic speed, and

δv is the variation in particle velocity. In Equation (3) and in air, the two terms alternate, with equal maxima. This is not the case here. In air, there is only one wave mode, while in plasma there are several. It seems that the first term must emphasize pressure, and therefore density fluctuations, and will therefore emphasize the ion acoustic mode. It seems that the two terms can emphasize different modes and that the second term, the velocity energy, must emphasize the modes other than the ion acoustic mode. The other modes must also play some role in the first term. The second term will be discussed in Section 4.2. To evaluate the first term, the wave pressure energy at its maximum value, a set of data from the 3DP experiment (Lin et al. 1995) on the *Wind* mission is used. These data are labeled WI_EM_3DP and WI_PM_3DP for the particle pressures and WI_H0_MFI for the magnetic field, in CDAWeb. The purpose here is to evaluate the energy in ion acoustic waves, and the pressure is expected to follow the plasma density. The heating and the damping rate of the waves, which is the imaginary part of the frequency, depends on frequency so a set of measurements of some length must be used both to establish the average density and to establish the spectrum by Fourier transform. On the other hand, the presence of an average pressure in δp of the expression requires that the set not be too long, as then it might include effects such as discontinuities, compression regions, Langmuir waves from Type III bursts, etc., which would distort the results. This approach cannot lead to precise results. δp, the deviation from an average density, would be easy for the atmosphere, but the solar wind consists of many different plasmas, separated by current sheets and discontinuities. The choice of length is a compromise and limits the accuracy of the estimates.

As the calculations of Equation (3) are to be compared with direct measurements, particularly those of Coleman (1968), a period in 2005 which is at the same phase of the solar cycle as was *Mariner II* and Coleman's measurement has been chosen for the present analysis. A period of 14 hr, from 2005 February 17 10:00 to 24:00 was chosen, but then another period 2005 February 5 09:00 to 2005 February 5 24:00 was added. The first period was chosen at random, but it was found that the ion pressure was unusually large, and the second period was found by hunting for a period of low pressure. During most of these periods, the solar wind was slow, though some faster wind is found. During the *Mariner II* mission, from which important data will be used, there was an appreciable fraction of fast solar wind.

Figure 2 shows a spectrogram of the wave energy during the high pressure period. The data are presented to show the exponent of the power. The average wave energy of a single observation over the whole period is $4.07 \times 10^{-13}\,\mathrm{J\,m^{-3}}$. These data may be fitted with power $3.6 \times 10^{-15}\, f^{(-0.90)}$, shown as a red line. As it is known that the spectrum of density follows a $-5/3$ power law (Chen et al. 2013, Chen et al. 2014) an exponent of -0.9 might cast some doubt on the identification of pressure as being due to ion acoustic waves. It seems there must be some correlation between density and temperature. This is shown in Figure 3, for the two high and low pressure periods. The red curves are the expressions $4.8\ \rho^{0.105}$ for electrons and $4.6\ \rho^{0.56}$ for protons for the high pressure period, February 17. For the low pressure period, February 5, the curves are $3.0\ \rho^{0.31}$ for electrons and $4.6\ \rho^{0.53}$ for protons. It is expected that there be

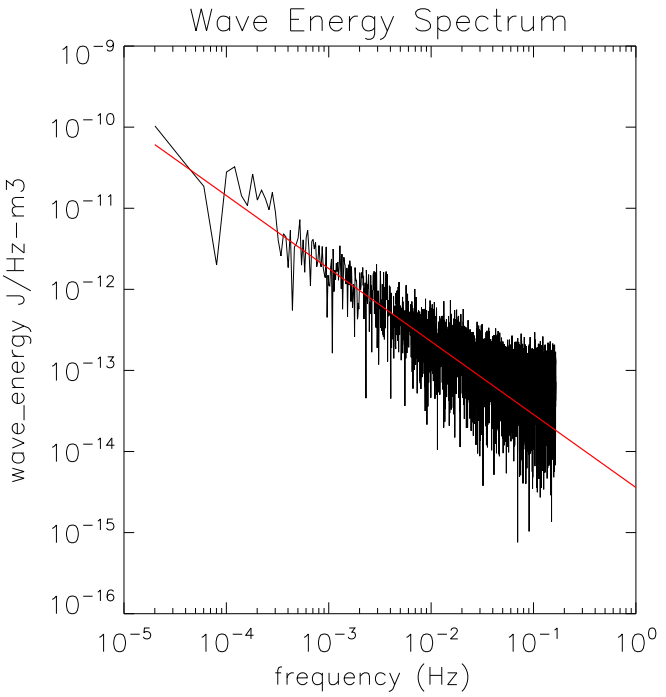

Figure 2. The spectrum of wave energy for the high ion pressure period. The red line represents the spectrum as $f^{(-0.80)}$.

some difference between the exponents for electrons and ions, as the γ's, the exponents, are often taken to be 3 for ions and 1 for electrons, but neither is found in this set. At any rate, the purpose here is to show that correlations alter the spectrum of wave energy from what might otherwise be expected to be similar to the density spectrum.

For further work, sets of 128 single observations are chosen. The time for such a set, 128 times the observation cadence of 3.04 s, is 389 s, fairly close to the 300 s samples used by Howes et al. (2012). The wave energies and the spectrum in each set are then evaluated from Equation (3) and from a fast Fourier transform of the 389 s of wave energy. The heating rate involves the damping, the imaginary part of the frequency. It is therefore necessary to calculate the heating in the frequency domain, rather than the time domain. The heating is found from a convolution of the power spectrum and the imaginary part of the wave frequency from the Fourier transform of the spectrum in each 389 s sample, taken here as real part/4 as the frequency is the observed, as discussed below. The Fourier inverse of the convolution is then a set of 128 measurements of the heating.

In this development, ω is the angular frequency in the rest frame of the plasma, whereas the measurements to be used are often the observed frequency in the moving solar wind, which according to the Taylor hypothesis is $\omega_{\mathrm{obs}} = k_{\|\mathrm{v}} v_{\mathrm{sw}}$. $k_{\|\mathrm{v}}$ is the component of the wave vector in the direction of the solar wind. As $k_{\|\mathrm{v}}$ is not measured, we use $k_{\|\mathrm{v}} = 2\pi f_{\mathrm{obs}}/\mathrm{Vsw}$ and also assume the dispersion relation for ion acoustic waves $\omega = k_{\|\mathrm{B}} V_{\mathrm{S}}$ where V_{S} is the ion sound speed and $\sqrt{((k_{\mathrm{B}}\mathrm{Te} + 3k_{\mathrm{B}}\mathrm{Tp})/M_{\mathrm{p}})}$ and $k_{\|\mathrm{B}}$ are the components of the wave vector in the direction of B.

The relation between f_{obs} and ω is then $f_{\mathrm{obs}} = (1/2\pi)(V_{\mathrm{sw}}/V_{\mathrm{s}})\omega$. For both of the periods analyzed, the solar wind speed was within $20\,\mathrm{km\ s^{-1}}$ of $V_{\mathrm{sw}} = 390\,\mathrm{km\,s^{-1}}$, and this was used for the connection between f and ω. Commonly in the data, $V_{\mathrm{s}} \sim 80\,\mathrm{km\,s^{-1}}$, but the actual value was used in the calculations.

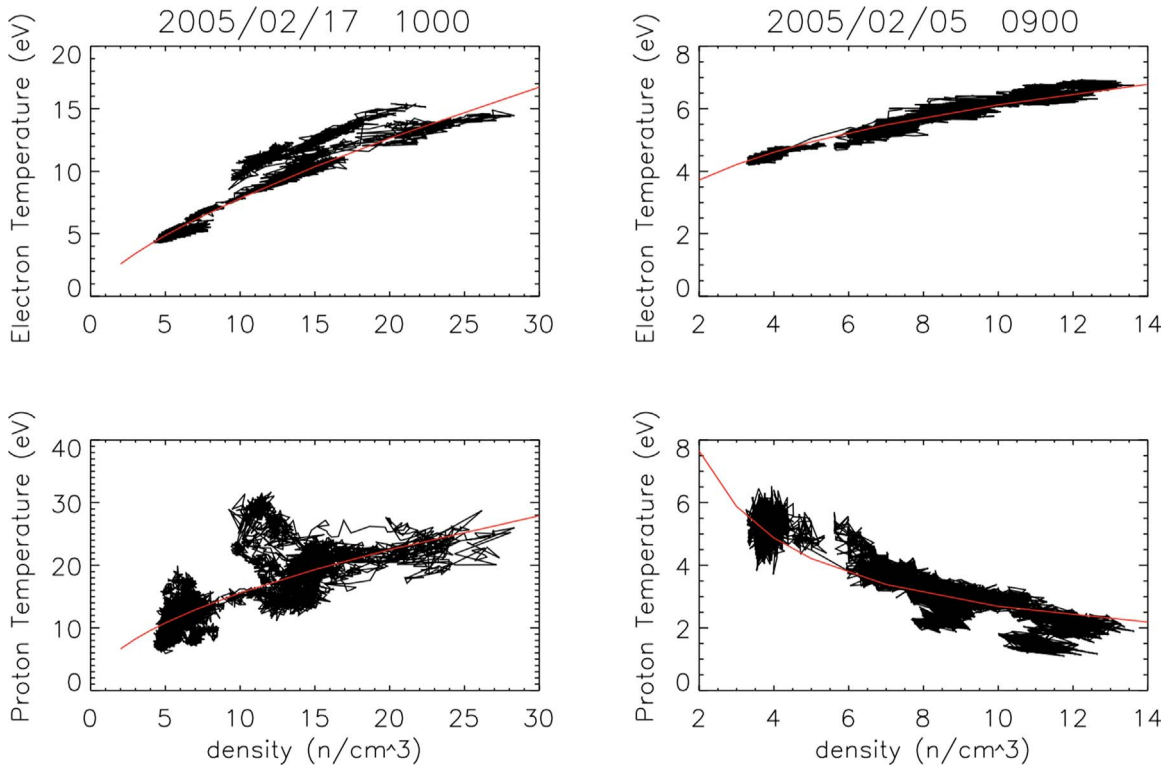

Figure 3. Particle temperature vs. density for the high pressure and the low pressure periods.

This typical value gives the ratio, $f_{obs}/\omega = 0.8$, not much different from unity. On the average then, the damping is approximately $f/4\,s^{-1}$, and this was used in the calculations of heating presented here.

The results of this calculation of heating are shown in Figure 4 for the low and high pressure periods. The horizontal lines in these figures are the heating rates found by Coleman (1968) and by Gazis & Lazarus (1982), to be discussed next.

This heating has been calculated for 389 s samples and corresponds to a part of the spectrum therefore from $1/389 = 0.00286$ to 0.16 Hz. In Section 4.2 a different way of attempting the energy calculation is discussed which is very sensitive to the lower limit on the frequency used. That is not the case here. The power law shown in Figure 2 is $f^{-0.9}$. Convoluting with damping proportional to f means that the heating spectrum has a dependence $f^{0.1}$, i.e., it is nearly flat with a slight increase toward higher frequencies. It is generally thought that the inertial spectrum, extends to about 0.2–0.4 Hz (Leamon 1998; Markovskii et al. 2008). A flat spectrum, integrated over the whole frequency range of the inertial region from $f = 10$ to 5 Hz to the Nyquist frequency of 0.4 Hz would be larger but not by an amount which is significant in view of the rather large uncertainties of this work.

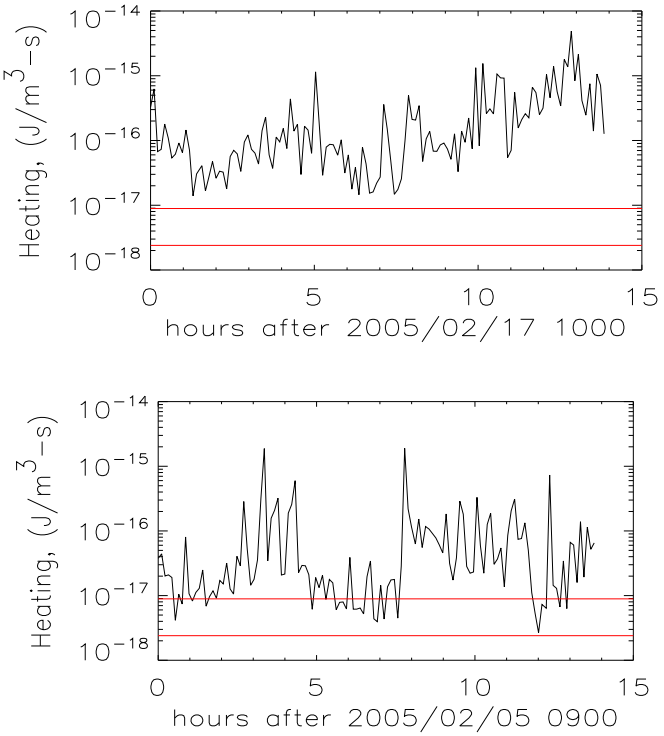

Figure 4. The heating rates, in J m^{-3} s^{-1} for the two periods studied, together with the heating rates found by Coleman (1968) near 1 au and Gazis & Lazarus (1982) beyond 1 au as red lines.

4. Comparison with Observations

4.1. Direct Observations of Heating

Coleman (1968) found the heating of protons required 2.4×10^6 erg g^{-1} s^{-1}. For the observed average density of 5.6 ions cm^{-3} or 9.4×10^{-21} kg m^{-3} this heating is 2.2–18 J m^{-3} s^{-1}. This measurement is from the *Mariner II* mission, between Venus and the Earth.

More recently, heating has been obtained by fitting data from temperature, T, as a function of distance from the Sun, R:

$$T(R) = T_0(R/R_0)^{-\alpha} \quad (4)$$

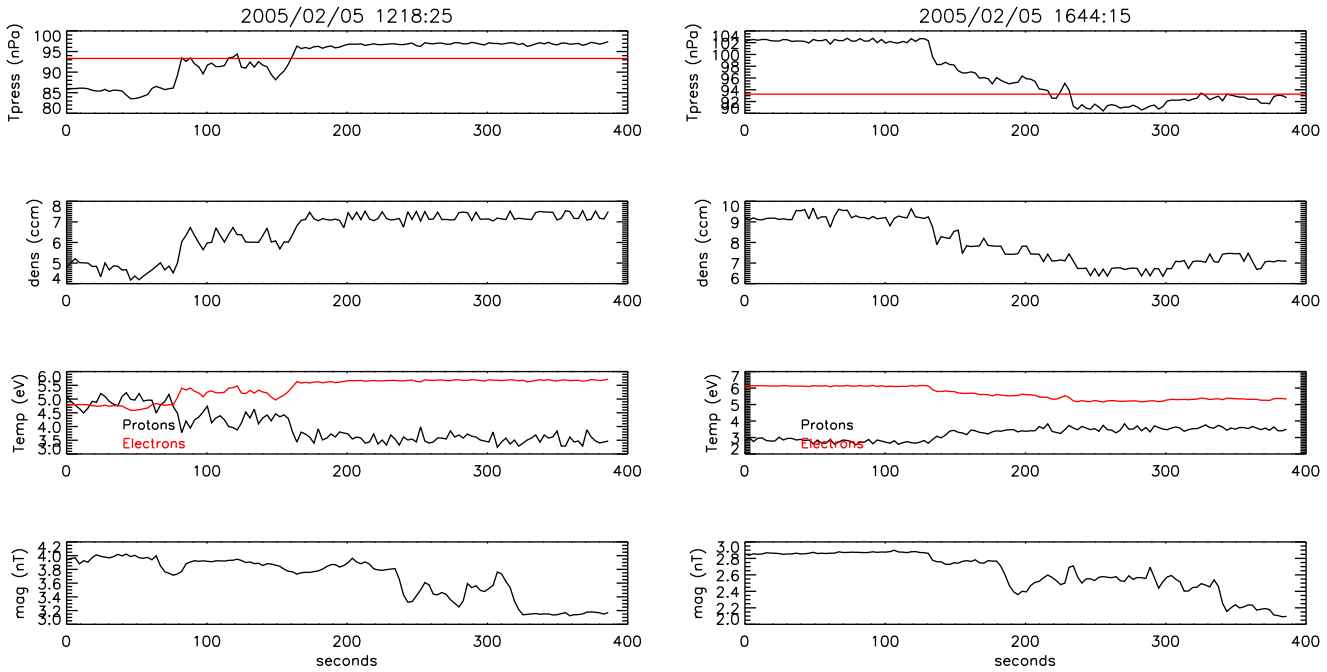

Figure 5. Pressure, density, temperature (eV), and magnetic field for two heating peaks. Also shown is a line for the average pressure, important in calculating the wave energy.

with various values of α. Typical is $\alpha = 0.7$ (e.g., Gazis & Lazarus 1982) For adiabatic cooling without other heating, $\alpha = 4/3$. For heating H J s^{-1} per particle, the evolution of k_BT would be: $k_BT/dR = (1/V_{SW})$, $k_BT/dt = H/V_{SW}$, with the consequence that the heating per proton required to maintain a temperature exponent α is

$$H = k_BT(4/3 - \alpha)V_{SW/R}. \quad (5)$$

For $\alpha = 7$, $V_{SW} = 450$ km s^{-1}, $k_BT = 5$ eV, and $R = 1$ au, this implies 9.9×10^{-6} eV s^{-1} per s-proton, or 8.9×10^{-18} J m^{-3} for the *Mariner* density. This is about four times higher than Coleman (1968).

The best mission for the study of heating within 1 au is the *Helios* mission. The *Helios* data have been recently reworked by Stansby et al. (2018) with different values of α for different components of the solar wind. The values are generally between 0.7 and 1, in accordance with the results above.

The horizontal lines in Figure 4 show these measurements of heating, with the Coleman measurements being the lower. It can be seen that the calculated heating is frequently larger, sometimes one or two orders of magnitude larger than the observations. Three reasons have been found which account for this overestimate.

First, a part of this discrepancy is wave mixture. In this work, no certain identification has been made of ion acoustic waves. It is only thought that using the pressure part of Rayleigh's formula will be inclined toward ion acoustic waves. There is undoubtedly some mixture of other modes in the signal, and the calculation here assumes that all of the wave energy, without distinction as to mode, is delivered to particles on the timescale of ion acoustic damping. This leads to an unavoidable overestimate. As a partial indication of the presence of other modes, the correlation between the magnitude of the magnetic field and the density has been calculated for each 389 s set. A negative correlation is generally taken as representing ion acoustic waves. For the low pressure set, 66 of the correlations were negative and 62 were positive. For the high pressure set, the numbers were, surprisingly, the same. This is taken as indication that mixing of other modes is considerable but that an appreciable fraction of the wave energy is due to ion acoustic waves. Of the three causes of the overestimate, this mixing could be estimated as 50% and is probably the least important.

Second, it is interesting to investigate the very large peaks seen, far above the observed heating, especially in the low pressure set. Figure 5 shows some plasma parameters for two large peaks. On the left are parameters for the peak at 7.8 hr in Figure 4. For this large peak, the density–magnetic field correlation is negative, −0.63, as can be seen, indicating a major component of ion acoustic waves. On the right are the parameters of the largest peak at 3.45 hr. The density–magnetic field correlation is positive, +0.76, indicating a large component of shear Alfvén waves. These are both boundaries between two different plasmas. It is assumed that these are the familiar rotational and tangential discontinuities, boundaries between plasmas of different characteristics. There is no other easy distinguishing characteristic of the two, and it seems that the peaks are simply due to very large apparent wave energy that is a consequence of the large pressure change. This is just the situation that it was attempted to avoid by choosing short sections to be analyzed, but as is seen, it was sometimes not successful. The calculation program automatically assigns a heating of $f/4$ to these, but, of course, the energy is not due to waves that are the interest of this work.

Third, in the calculation of heating the expression for damping has been used which is appropriate for wave propagation parallel to the magnetic field. As pointed out by Narita & Marsch (2015), the damping of ion acoustic waves becomes much less for oblique propagation. Figure 6 shows the ratio of imaginary part of the frequency to the real part as a function of theta, the angle between the wave vector and the magnetic field, from a Vlasov calculation. The plasma parameters have been taken from a period in the

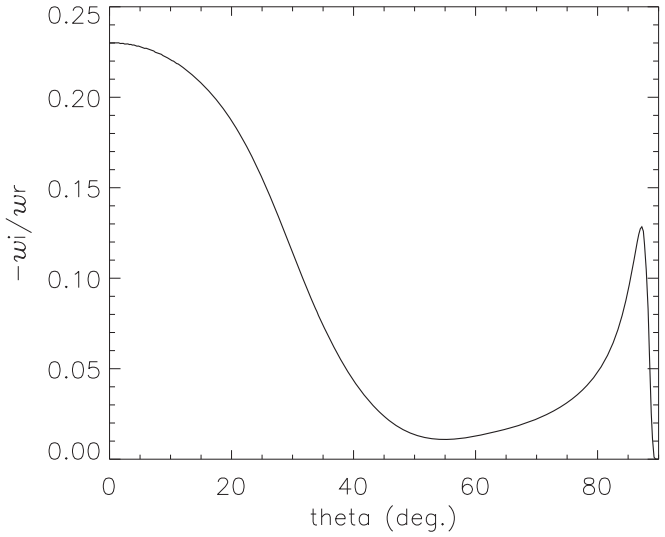

Figure 6. Ratio of the imaginary part of the frequency to the real part as a function of angle theta between the wave vector and the magnetic field. Plasma parameters are for a period during the low pressure set.

middle of the low pressure set, and for a frequency midway between the extremes of a 389 s period. It has been known for a long time that the cascade favors strongly oblique daughters of the cascade processes (Sridhar & Goldreich 1994; Goldreich & Sridhar 1995). The lowest damping in Figure 6 is $-\omega i/\omega r = 0.011 = 1/91$. If $\omega/91$ is used for the damping in Figure 5 instead of $\omega/4$, the heating, except for the highest peaks, falls below the observations. Figure 7 shows a recalculation of the high pressure study using this slower damping, resulting in the worst discrepancy. It can be seen that the allowed range of oblique damping would allow an obliquity, giving full agreement with the observations.

There are then three causes of the overestimates shown in Figure 4: mixing of other modes, mixing of different plasmas, and reduced damping of oblique ion acoustic waves. In accounting for these, it seems that the damping of ion acoustic-kinetic slow mode waves can provide most or nearly all of the observed heating.

4.2. Wave Energy from Electric Field Spectra

The second term in the Rayleigh formula, Equation (3), might also be used to evaluate the heating. The particles' velocities are due to the electric fields of the waves. Accordingly:

$$dv/dt = eE/m \qquad \delta v = eE(\omega)/(m\omega).$$

These two parts of the second term, the kinetic energy of the different particles, is clearly dominated by the electron part, so dropping ions in what follows,

$$dv/dt = eE/m_e \qquad \delta v = eE(\omega)/(m_e\omega), \tag{6}$$

gives for the energy per unit volume and frequency range:

$$dW_j(\omega, k)/dVd\omega = (n/2m_e)(eE(\omega)/\omega)^2 = 7.10^{-2}\langle E(\omega)/\omega)\rangle^2 \mathrm{J\ m^{-3}}\delta\omega. \tag{7}$$

In this, the particle density for each species has been taken as 5×10^6 in correspondence with other evaluations used in this work.

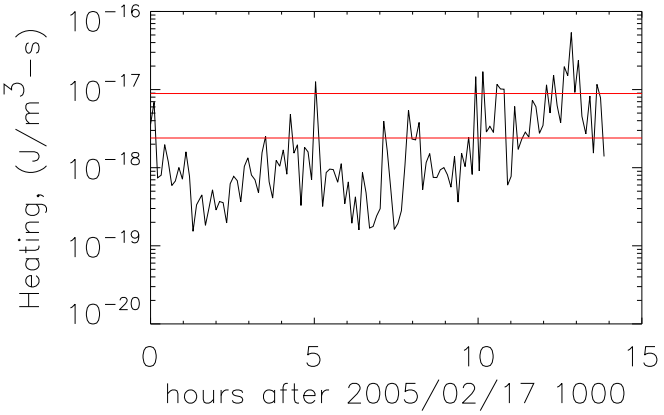

Figure 7. Calculated and observed heating for a section of the high pressure set, using the lowest damping from Figure 6.

In the ion acoustic slow mode, the ion and electron densities are very close to equal and the electric fields are small. Consequently, the energy of the particles is considerably larger than that of the fields, and the coefficient of $\langle E^2\rangle$ in the energy is large. The coefficient of the electric field energy is then:

$$2(n/2m_j)(e/\omega)^2/\varepsilon_0 = 1.6 \times 10^{10}/\omega^2. \tag{8}$$

This is, as stated above, very large and increases toward lower frequency.

Measurements of the electric field spectrum are usually reported as

$$\langle E^2(f_{obs})\rangle = A_E f^{-\alpha}\,(\mathrm{V/m})^2/\mathrm{Hz}.$$

The wave energy spectral density $dW(\omega,k)/dVd\omega$ is then

$$dW_j(\omega, k)/dV - df = (ne^2/2m_e)(1/2\pi)V_{sw}/V_s)^{-\alpha-2} \times (A_E f^{-\alpha-2}) = 0.6(A_E f^{-\alpha-2}).$$

In this, the V_{sw}/V_s etc. factor has been evaluated for $a = 5/3$ and the subscript on f dropped. The total energy is then obtained by integrating the frequency spectrum over a range from f_{low} to f_{high}. If f_{high} is reasonably far above f_{low}, it may be ignored. However, what is desired here is the heating rate, i.e., the rate at which this energy is transferred to the plasma. This rate is given by the rate of decay of ion acoustic waves, approximately a third to a half of the real part of the frequency, $\omega = f/1.8$, so that the heating, H, in joules per cubic meters per second, again integrating over the frequency spectrum, is:

$$H = 0.22(A_E f_{low}^{-\alpha-1}).$$

Kellogg et al. (2006) found $A_E f^{-\alpha} = 10^{-10} f^{-5/3}\ (\mathrm{V/m})^2\ \mathrm{Hz}^{-1}$, Bale et al. (2005) found $8 \times 10^{-10} f^{-5/3}$.

For the Kellogg et al. spectrum: $H = 6 \times 10^{-11}\ f_{low}^{-\alpha-1}$ $\mathrm{J\,m^{-3}\,s^{-1}}$. This result critically depends, as can be seen, on the lower limit of the ion acoustic wave spectrum which in not known. Published measurements of the electric field spectrum do not show any break that might be interpreted as a change of mode. For example, Chen et al. (2011) show a spectrum with a break at about 2×10^{-5} Hz which corresponds roughly to the break in the magnetic field spectrum corresponding to the lower limit of the inertial region. A more direct measurement that might be interpreted as the lower limit of ion acoustic waves could come from Vellante & Lazarus (1987), who investigated the correlation between B and density down to 1.6×10^{-4} Hz

(period 2 hr). A lower estimate due to Goldstein & Siscoe (1972) is quoted by Tu & Marsch (1995) (p 120), as between 2.6×10^{-3} and 4×10^{-5} Hz (7 hr). However, even if the rather high lower limit of 2.6×10^{-3} Hz corresponding to the lower limit of the 389 s samples used for the pressure heating, the result is enormously greater than the observations. It seems that this large electric field must come from a part of the electric field spectrum due to shear Alfvén waves or a whistler mode, which have only a very slow decay, especially at low frequencies, and so do not contribute much to the heating. It also suggests that the calculations above from pressure measurement may sometimes be too large because there may be some Alfvén waves in the spectrum. In any case, this estimate from the second Rayleigh term is much larger than that from the pressure term and must be dominated by other waves.

5. Summary and Conclusions

It seems that, within the uncertainties of these calculations, the heating of the solar wind by absorption of ion acoustic-kinetic slow mode waves is a significant part and perhaps nearly all of the observed heating of the solar wind in the regions reached before the *Parker Solar Probe*mission. This verifies the early suggestions of Tu & Marsch (1994, 1995), and Howes et al. (2012) that the ubiquitous density fluctuations are in the ion acoustic-kinetic slow mode and the decay of these provides heating of the solar wind. This does not contradict the longstanding belief that the heating is due to magnetic field turbulence. (For a review of the enormous literature on this subject see Usmanov et al. 2011.) The ion acoustic waves must be just a step in the conversion of turbulence to heat, and the generation of these short duration waves from the turbulence remains to be understood. A suggestion, but at higher frequency and in the fast wind, was made by Jiling (1999). Some progress has been made, algebraically by Derby (1978) and Goldstein (1978), observationally by Bowen et al. (2018), and in simulations by Matteini et al. (2010), but understanding is not yet complete.

Ion acoustic waves are generated, more or less, as a byproduct used to balance the energy and momentum conservation requirements, in a range of nonlinear plasma processes (see references immediately above and also others (Forslund et al. 1972; Hasegawa & Chen 1975, 1976; Lee 1974; Chen 1977)). The relative importance of these, and perhaps others not yet described, remain an important subject of research, both at 1 au and for *Parker Solar Probe* closer to the Sun.

This work was supported by the National Aeronautics and Space Administration under grant NNX14AK73G.

The author thanks CDAWeb and S.D. Bale and R.P. Lin for the pressure and plasma density data. Thanks to CDAWeb and R. Lepping for the magnetic field data. Thanks also to Greg Howes, (University of Iowa), Kris Klein (now at University of Arizona) and Marco Velli (University of California at Los Angeles) for helpful discussions. Thanks also to OMNIweb plus, Natalia Papitashvili and Marcia Neugebauer for the solar wind speed data from the *Mariner II* mission.

The data used in this work are available to the public either from the National Space Science Data Center or from published data.

ORCID iDs

Paul J. Kellogg https://orcid.org/0000-0001-5223-689X

References

Auerbach, S. P. 1979, PhFl, 22, 1650
Bale, S. D., Kellogg, P. J., Mozer, F. S., Horbury, T. S., & Reme, H. 2005, PhRvL, 94, 215002
Barnes, A. 1966, PhFl, 9, 1483
Bowen, T. A., Badman, S., Hellinger, P., & Bale, S. D. 2018, ApJL, 854, L33
Brillouin, L. 1921, Comptes rendus hebdomadaires des séances de l'Académie des Sciences, 173, 1167
Burlaga, L. E., & Ogilvie, K. W. 1970a, ApJ, 159, 659
Burlaga, L. E., & Ogilvie, K. W. 1970b, SoPh, 15, 61
Chen, C. H. K., Bale, S. D., Salem, C., & Mozer, F. S. 2011, ApJL, 737, L41
Chen, C. H. K., Howes, G. G., Bonnell, J. W., et al. 2013, in AIP Conf. Proc. 1539, SOLAR WIND 13: Proc. of the Thirteenth Int. Solar Wind Conf., ed. G. P. Zank et al. (Melville, NY), 143
Chen, C. H. K., Sorriso-Valvo, L., Šafránková, J., & Němeček, Z. 2014, ApJL, 789, L8
Chen, L. 1977, PlPh, 19, 47
Coleman, P. J., Jr. 1968, ApJ, 153, 371
Derby, N. F., Jr. 1978, ApJ, 224, 1013
Forslund, D. W., Kindel, J. M., & Lindman, E. L. 1972, PhRvL, 29, 249
Fried, B. D., & Conte, S. D. 1961, The Plasma Dispersion Function (New York: Academic)
Gazis, P. R., & Lazarus, A. J. 1982, GeoRL, 9, 431
Goldreich, P., & Sridhar, S. 1995, ApJ, 438, 763
Goldstein, B., & Siscoe, G. L. 1972, in Solar Wind, ed. C. P. Sonett et al. (Washington, DC: NASA), 506
Goldstein, M. L. 1978, ApJ, 219, 700
Hasegawa, A., & Chen, L. 1975, PhRvL, 35, 370
Hasegawa, A., & Chen, L. 1976, PhRvL, 36, 1362
Howes, G. G., Bale, S. D., Klein, K. G., et al. 2012, ApJL, 753, L19
Howes, G. G., Cowley, S. C., Dorland, W., et al. 2006, ApJ, 651, 590
Jiling, H. 1999, SoPh, 185, 391
Kellogg, P. J., Bale, S. D., Mozer, F. S., Horbury, T. S., & Reme, H. 2006, ApJ, 645, 704
Kellogg, P. J., & Horbury, T. S. 2005, AnGeo, 23, 3765
Landau, L. D., & Lifshitz, E. 1960, Electrodynamics of Continuous Media (1st ed.; Oxford, New York: Pergamon)
Landau, L. D., & Lifshitz, E. 1969, Electrodynamique des Milieux Continus (Moscow: Editions Mir)
Leamon, R. J. 1998, JGR, 103, 4775
Lee, K. F. 1974, PhFl, 17, 1343
Lepping, R. P., Acũna, M. H., Burlaga, L. F., Scheifele, J., & Worley, E. M. 1995, SSRv, 71, 207
Lin, R. P., Anderson, K. A., Ashford, S., Ronnet, J. C., & Paschmann, G. 1995, SSRv, 71, 125
Markovskii, S. A., Vasquez, B. J., & Smith, C. W. 2008, ApJ, 675, 1576
Matteini, L., Landi, S., Velli, M., & Hellinger, P. 2010, JGRA, 115, A09106
Narita, Y., & Marsch, E. 2015, ApJ, 805, 24
Parker, J. T., Highcock, E. G., Schekochihin, A. A., & Dellar, P. J. 2016, PhPl, 23, 070703
Rayleigh, L., & Strutt, J. W. 1894, The Theory of Sound (New York: Dover), 19
Schekochihin, A. A., Cowley, S. C., Dorland, W., et al. 2009, ApJS, 182, 310
Sridhar, S., & Goldreich, P. 1994, ApJ, 432, 612
Stansby, D., Salem, C., Matteini, L., & Horbury, T. 2018, SoPh, 293, 155
Stix, T. H. 1962, The Theory of Plasma Waves (New York: McGraw-Hill)
Stix, T. H. 1992, Waves in Plasmas (New York: AIP)
Tu, C.-Y., & Marsch, E. 1994, JGR, 99, 21481
Tu, C.-Y., & Marsch, E. 1995, SSRv, 73, 1
Usmanov, A. V., Matthaeus, W. H., Breech, B. A., & Goldstein, M. L. 2011, ApJ, 727, 84
Vasquez, B. J., & Hollweg, J. V. 1999, JGRA, 104, 4681
Vellante, M., & Lazarus, A. J. 1987, JGR, 92, 9893
Verscharen, D., Chen, C. H. K., & Wicks, R. T. 2017, ApJ, 840, 106
Yao, S., He, J.-S., Marsch, E., et al. 2011, ApJ, 728, 146